Production of Characteristic X Rays by Low-Energy Protons

R. C. JOPSON, HANS MARK, AND C. D. SWIFT
Lawrence Radiation Laboratory, University of California, Livermore, California
(Received February 2, 1962; revised manuscript received May 21, 1962)

The cross sections for the production of characteristic x rays emitted by targets bombarded with low-energy protons have been measured for a number of elements. Scintillation counters capable of resolving x rays with quantum energies as low as 2 keV were used as detectors. X rays from K, L, and M shells were observed and the behavior of the production cross section for these was measured as a function of incident proton energy. Proton beams with energies between 100 and 500 keV produced by the Lawrence Radiation Laboratory (LRL) Cockcroft-Walton accelerator were used for the bombardments. The ionization cross sections for the shells have also been computed using measured or extrapolated values of the appropriate fluorescence yields. The experimental results for K-shell ionization are in good agreement with previous measurements for a number of elements. The dependence of the K-shell ionization cross section on atomic number (Z) and on the energy of the bombarding protons is also in accord with the theoretical predictions provided that the deflection of the bombarding particle by the Coulomb field of the nucleus is taken into account. The measured L-shell ionization cross sections are smaller than the values predicted by a Born approximation calculation in which Coulomb effects are neglected. No calculations are available for M-shell ionization cross sections so only a qualitative explanation of their behavior is presented.

I. INTRODUCTION

ATOMIC ionization by heavy, high-speed ions has long been a field for experimental study.[1] Extensive measurements of the energy losses suffered by charged particles passing through matter have been made. These experiments determine an average atomic ionization cross section and also average atomic ionization potentials.[2] Another approach is to measure separately the ionization cross sections of the various atomic shells. This is done by observing the characteristic radiations emitted whenever an ionization event occurs. The recent development of scintillation detectors capable of detecting and resolving x rays in the region of 10-keV quantum energy and below has revived interest in such measurements. Characteristic x rays produced by low-energy protons have been observed by a number of different workers.[3] More recently, Lewis, Simmons, and Merzbacher[4] and Bernstein and Lewis[5] measured the production cross sections for K and L x rays in a number of elements using protons with bombarding energies from 1.0 to 4.0 MeV. Simane and Urbanec,[6] B. Singh,[7] Jamnik and Zupančič,[8] and S. Messelt[9] all have performed and described experiments on the K-shell ionization cross sections for many elements using incident proton energies as low as 0.250 MeV. Such measurements will be compared with the present results wherever possible. The present work describes an extension of this work to L- and M-shell ionization cross sections for a number of elements at lower proton bombarding energies.

A number of extensive theoretical treatments of the atomic ionization process by proton bombardment are available. The initial work of Bethe,[10] Henneberg,[11] and Hönl[12] was done in connection with computing stopping powers. This work, together with more recent treatments, is summarized in a review article by Merzbacher and Lewis.[13] In all of these calculations, the ionization cross section is computed using the Born approximation in which plane waves are used to describe the incoming and outgoing protons. The Coulomb interaction between the incoming proton and the atomic electron ejected during the collision is used as the perturbation for which the matrix elements are calculated. The work of Messelt[9] indicated that the Born-approximation calculations predict K-shell ionization cross sections which are larger than the observed values at low ($\sim$ few hundred keV) bombarding energies. In this case, the plane-wave representation of the incoming and outgoing proton is inadequate, since the deflection of the bombarding particle by the Coulomb field of the nucleus must also be considered. A semiclassical treatment of this effect exists[14] and the results of this calculation are in good agreement with Messelt's measurements[9] and those given in this paper.

The L-shell ionization cross sections have also been computed using the plane wave Born approximation.[13,15,16] The theoretical ionization cross sections

[1] N. Bohr, Phil. Mag **25**, 10 (1913).
[2] See, for example, J. Lindhard and M. Scharff, Kgl. Danske Videnskab. Selskab, Mat-fys. Medd. **27**, No. 15 (1953); and W. Whaling, *Nuclear Spectroscopy* (Academic Press Inc., New York, 1960), Part A, Chap. I.
[3] W. Bothe and H. Franz, Z. Physik **52**, 466 (1928); C. Gerthsen and W. Reusse, Physik. Z. **34**, 478 (1933); and M. S. Livingston, F. Genevese, and E. Konopinski, Phys. Rev. **51**, 835 (1937).
[4] H. W. Lewis, B. E. Simmons, and E. Merzbacher, Phys. Rev. **91**, 943 (1953).
[5] E. M. Bernstein and H. W. Lewis, Phys. Rev. **95**, 83 (1954).
[6] C. Simane and J. Urbanec, Czech. J. Phys. **5**, 40 (1955).
[7] B. Singh, Phys. Rev. **107**, 711 (1957).
[8] D. Jamnik and Č. Zupančič, Kgl. Danske Videnskab. Selskab, Mat-fys. Medd. **31**, No. 2 (1956).
[9] S. Messelt, Nuclear Phys. **5**, 435 (1958).
[10] H. A. Bethe, Ann. Physik **5**, 325 (1930).
[11] W. Henneberg, Z. Physik **86**, 592 (1933).
[12] H. Hönl, Z. Physik **84**, 1 (1933).
[13] E. Merzbacher and H. W. Lewis, *Encyclopedia of Physics* (Springer-Verlag, Berlin, 1958), Vol. 34, p. 166.
[14] J. Bang and J. M. Hansteen, Kgl. Danske Videnskab. Selskab, Mat-fys. Medd. **31**, No. 13 (1959).
[15] M. C. Walske, Phys. Rev. **101**, 940 (1956).
[16] M. V. Mihailovic, "J. Stefan" Inst. Repts (Ljubljana) **3**, 55 (1956).

computed in this way are considerably larger than the experimental values at incident proton energies near 5 MeV. It is very likely that it is also necessary to include Coulomb deflection effects if the L-shell cross sections are to be correctly predicted. No estimates of the M-shell ionization cross sections are available so that no quantitative comparison with the present experiments can be made.

II. EXPERIMENTAL METHODS

The Cockcroft-Walton accelerator at LRL, Livermore, was used to provide the proton beams. This machine is capable of delivering proton beams of up to 100 μA continuously variable in energy between 100 and 500 keV. The particles, after acceleration, are passed through a 25° bending magnet to insure that the beam which strikes the target is isotopically pure.

The experimental geometry is very similar to that described in Fig. 1 of reference 5. A target is mounted at a 45° angle to the beam direction and the x-ray counter is placed at right angles to the beam. The x rays produced at the target are passed through a thin (0.001-in.) Mylar window to minimize absorption effects. Thick targets (that is, targets in which the proton beam is completely stopped) were used in all of these experiments. Whenever possible, solid metallic targets were employed. In many cases, however, the elements were either nonmetals or were not available in solid metallic form. In some instances, finely powdered (100-mesh or smaller) metals were pressed into small depressions on lead backing discs. These made satisfactory targets, however, the x-ray yield from such a powdered target was generally somewhat lower than that obtained from the solid metal target made of the same material. An experimentally determined correction factor ($f=1.2$) was used to multiply the observed counting rates in order to obtain the values used to compute the cross sections.

In some cases, only oxides of the desired target materials were available. These materials (mainly rare-earth oxides) were also obtained in fine-mesh form and pressed into lead or brass backing discs by an arbor press using pressures of the order of 5000 psi. When such targets were bombarded with proton beams, very high backgrounds of low energy (about 1 keV probably) x rays with a more-or-less continuous spectrum were observed in the x-ray detector. These oxides are excellent insulators. When they are bombarded with relatively high-energy protons, regions of very high charge density and hence field strengths could be created. These large electric fields would cause breakdown phenomena in which large numbers of low-energy photons are emitted. That this explanation is very probably correct was demonstrated by adding a small amount of finely divided conducting material to the powdered oxide. The effect disappeared when this was done and, in practice, the target material (rare-earth oxide) was, therefore, mixed with 5% by weight of aluminum powder.

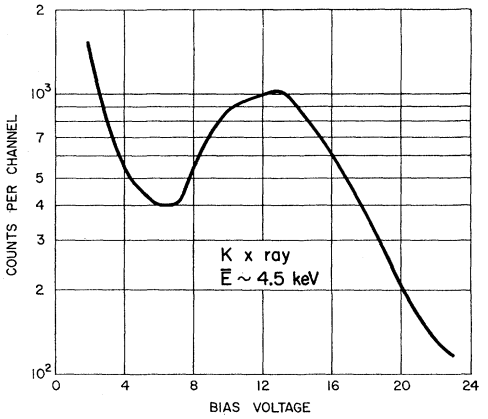

FIG. 1. The x-ray spectrum observed when a thick titanium target is bombarded with 441-keV protons is shown. The width of the peak is not a good measure of the counter resolution since there are several unresolved K x-ray components in the observed peak.

Finally, two of the targets (Gd, Yb) were made by evaporating the material on a copper backing disc. It is quite difficult to arrive at a reasonable estimate of the true x-ray yield from evaporated targets. The targets were sufficiently thick so that all the protons stopped in the rare-earth layer since no characteristic x rays from the copper backing were observed. The composition of the coating cannot be determined easily, since it is probably partially oxidized.

The yields from evaporated targets and pressed oxide targets made of the same rare earths (Er and Tm) were compared and a correction factor was determined. The yield from the oxide target was 16% lower than the yield from the evaporated target in both cases. The

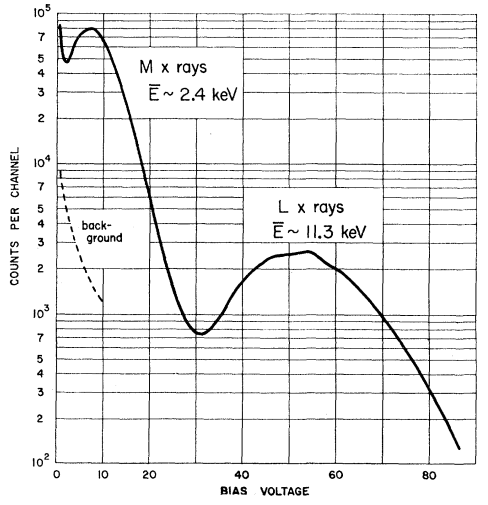

FIG. 2. The x-ray spectrum observed when a thick lead target is bombarded with 441-keV protons is shown. Peaks corresponding to both M and L x rays are observed. The background spectrum in the low-energy region is also shown.

TABLE I. X-ray yields. (Proton bombarding energy 441 keV.)

Element	Z	Atomic shell	X rays per μC, before geometrical and absorption corrections	Ω/A	(x rays/proton)	dN/dE (x rays/proton keV)
Uranium	92	M	74 500	3700	4.37×10^{-5}	3.25×10^{-7}
		L	228	1115	4.03×10^{-8}	4.15×10^{-10}
Bismuth	83	M	25 500	17 300	7.00×10^{-5}	3.18×10^{-7}
		L	2020	1040	3.33×10^{-7}	3.51×10^{-9}
Lead	82	M	23 300	23 800	8.81×10^{-5}	4.06×10^{-7}
		L	2310	1041	3.82×10^{-7}	4.02×10^{-9}
Mercury[a]	80	M	9540	47 600	7.21×10^{-5}	4.29×10^{-7}
		L	2510	1044	4.16×10^{-7}	4.69×10^{-9}
Gold	79	M	9180	73 200	1.07×10^{-4}	4.58×10^{-7}
		L	4510	1050	7.52×10^{-7}	7.57×10^{-9}
Platinum	78	M	6380	115 700	1.17×10^{-4}	5.11×10^{-7}
		L	5160	1050	8.60×10^{-7}	7.82×10^{-9}
Iridium[b]	77	L	5080	1055	1.02×10^{-6}	8.88×10^{-9}
Osmium[b]	76	L	7310	1069	1.49×10^{-6}	1.12×10^{-8}
Rhenium	75	L	8640	1079	1.48×10^{-6}	1.32×10^{-8}
Tungsten	74	L	9480	1090	1.64×10^{-6}	1.59×10^{-8}
Tantalum	73	L	11 300	1097	1.97×10^{-6}	1.67×10^{-8}
Hafnium	72	L	12 300	1105	2.16×10^{-6}	1.89×10^{-8}
Lutetium[a]	71	L	9580	1109	1.68×10^{-6}	1.50×10^{-8}
Ytterbium[a]	70	L	11 400	1120	2.03×10^{-6}	1.40×10^{-8}
Thulium[a]	69	L	12 100	1130	2.17×10^{-6}	1.58×10^{-8}
Erbium[a]	68	L	11 800	1142	2.14×10^{-6}	1.64×10^{-8}
Gadolinium[c]	64	L	19 200	1205	3.68×10^{-6}	2.77×10^{-8}
Barium[a]	56	L	36 100	1546	8.86×10^{-6}	5.60×10^{-8}
Tellurium[b]	52	L	76 000	1780	2.58×10^{-5}	1.61×10^{-7}
Cadmium	48	L	43 400	3600	2.48×10^{-5}	1.60×10^{-7}
Silver	47	L	70 700	4400	4.94×10^{-5}	2.91×10^{-7}
Molybdenum	42	L	17 300	26 400	7.23×10^{-5}	4.18×10^{-7}
		K	154	1024	2.50×10^{-8} (3.60×10^{-8})[d]	2.32×10^{-10}
Zirconium	40	L	5720	106 500	9.67×10^{-5}	5.23×10^{-7}
		K	240	1024	3.90×10^{-8}	3.70×10^{-10}
Copper	29	K	9410	1109	1.71×10^{-6}	1.47×10^{-8}
Iron	26	K	15 600	1205	2.98×10^{-6}	2.69×10^{-8}
Titanium	22	K	40 500	1546	9.92×10^{-6}	8.48×10^{-8}

[a] Pressed metallic oxide targets. [b] Pressed powdered metal target. [c] Evaporated target. [d] See reference 9.

yields from the Gd and Yb targets were, therefore, multiplied by this correction factor and the cross sections were computed, assuming pure oxide targets.

The proton beam currents on the target were measured by conventional methods, using a dc amplifier charge-rate meter. To prevent secondary electron emission either at the target or at the collimating slits from distorting the beam current measurement, a guard ring at a large negative potential (−1000 V) was placed in front of the target. The beam itself was focused on the target in a circular spot approximately 3/16 in. in diam. The error in the beam current measurements was approximately ±5%, the main source being electronic drift in the integrator circuit. This error was determined by periodically calibrating the integrator with a known current source.

Since the x-ray production cross sections depend rather strongly on the proton bombarding energy [see Eq. (3)], it is important to determine as accurately as possible the operating energy of the Cockcroft-Walton machine. Normally, this energy is measured by measuring the voltage across a calibrated dropping resistor placed between ground and the high-voltage terminal. This resistor is calibrated by using the machine to produce various nuclear reactions which have sharp resonances in the production cross sections. In the present work, γ rays from the $Li^7(p,\gamma)$ and $F^{19}(p,\alpha,\gamma)$ reactions were used.[17] The yield was determined as a function of proton energy using a thin, evaporated LiF target. This target was installed on a second extension of the beam pipe from the bending magnet, so that it was easy to make a spot check of the machine energy between each cross section determination.

The scintillation counters used in this set of experiments were similar to those employed in an earlier experiment.[18] Thin, cleaved NaI crystals were employed with 0.002 in. thick Be windows. The lowest quantum energy of the x rays which can be observed using these counters is about 2.5 keV, provided that the source is sufficiently intense. Figure 1 shows the spectrum when a Ti target is bombarded with 441-keV protons. The composite peak, with a mean energy of about 4.5 keV, is due to the K x-ray lines (K_{α_1}, K_{α_2}, etc.). Since the line consists of several components, the width of the peak is not an accurate measure of the crystal resolution. Figure 2 shows the spectrum from a lead target.

[17] F. Ajzenberg and T. Lauritsen, Revs. Modern Phys. **27**, 77 (1955).

[18] R. C. Jopson, H. Mark, C. D. Swift, and J. H. Zenger, Phys. Rev. **124**, 157 (1961).

TABLE II. X-ray production and atomic ionization cross sections. (Proton bombarding energy 441 keV.)

Element	Z	Atomic shell	$\bar{\mu}$ (cm²/g)	$S(E)$ [keV/(mg/cm²)]	σ_x (cm²)	Fluorescence yield	σ_I (cm²)
Uranium	92	M	1100	95	3.12×10^{-23}	0.06	5.2×10^{-22}
		L	94		1.68×10^{-26}	0.45	3.7×10^{-26}
Bismuth	83	M	1100	99	3.75×10^{-23}	0.04	9.4×10^{-22}
		L	94		1.31×10^{-25}	0.40	3.3×10^{-25}
Lead	82	M	1100	96	4.69×10^{-23}	0.04	1.2×10^{-21}
		L	98		1.46×10^{-25}	0.40	3.7×10^{-25}
Mercury	80	M	1072[a]	120[a]	4.76×10^{-23}	0.04	1.2×10^{-21}
		L	96[a]		2.23×10^{-25}	0.37[b]	6.0×10^{-25}
Gold	79	M	1100	93	5.24×10^{-23}	0.04	1.3×10^{-21}
		L	110		2.57×10^{-25}	0.31	8.3×10^{-25}
Platinum	78	M	1100	93	5.71×10^{-23}	0.04	1.4×10^{-21}
		L	115		2.67×10^{-25}	0.36[b]	7.4×10^{-25}
Iridium	77	L	120	93	3.02×10^{-25}	0.34[b]	8.9×10^{-25}
Osmium	76	L	125	93	3.88×10^{-25}	0.35	1.1×10^{-24}
Rhenium	75	L	130	93	4.38×10^{-25}	0.31	1.4×10^{-24}
Tungsten	74	L	135	93	5.18×10^{-25}	0.31	1.7×10^{-24}
Tantalum	73	L	140	93	5.49×10^{-25}	0.29[b]	1.9×10^{-24}
Hafnium	72	L	145	94	6.19×10^{-25}	0.25[b]	2.5×10^{-24}
Lutetium	71	L	126[a]	141[a]	8.43×10^{-25}	0.24	3.4×10^{-24}
Ytterbium	70	L	141[a]	130[a]	5.95×10^{-25}	0.23	2.5×10^{-24}
Thulium	69	L	138[a]	144[a]	9.06×10^{-25}	0.23	3.8×10^{-24}
Erbium	68	L	145[a]	146[a]	9.45×10^{-25}	0.23	4.1×10^{-24}
Gadolinium	64	L	180[a]	142[a]	1.19×10^{-24}	0.20	6.0×10^{-24}
Barium	56	L	266[a]	148[a]	2.71×10^{-24}	0.15	1.8×10^{-23}
Tellurium	52	L	350	131	6.37×10^{-24}	0.12	4.9×10^{-23}
Cadmium	48	L	420	139	6.08×10^{-24}	0.11	5.5×10^{-23}
Silver	47	L	430	144	1.13×10^{-23}	0.10	1.1×10^{-22}
Molybdenum	42	L	600	150	1.69×10^{-23}	0.067	2.5×10^{-22}
		K	20		5.62×10^{-27}	0.733	7.67×10^{-27} (1.73×10^{-26})[c]
Zirconium	40	L	680	154	2.21×10^{-23}	0.057	3.9×10^{-22}
		K	22		8.75×10^{-27}	0.696	1.26×10^{-26}
Copper	29	K	52	180	2.88×10^{-25}	0.393	7.35×10^{-25}
Iron	26	K	74	214	5.53×10^{-25}	0.293	1.89×10^{-24}
Titanium	22	K	100	230	1.63×10^{-24}	0.170	9.59×10^{-24}

[a] Computed for oxide targets. [b] See reference 27. [c] See reference 9.

In this case, both the M and the L x rays are visible at 2.4 and 11.5 keV, respectively. The background spectrum shown in Fig. 2 is primarily phototube noise. The scintillation counters were used with RCA 6810A photomultiplier tubes especially selected for low noise properties.

III. CALCULATION OF CROSS SECTIONS FROM COUNTING RATES

The x-ray production cross section can be computed from the thick-target yield using the formula derived in reference 4.

$$\sigma_x(E)=(1/n)(dN/dE)S(E)+(1/n)\bar{\mu}N(E). \quad (1)$$

In this expression, $\sigma_x(E)$ is the cross section in cm², n is the number of target atoms per gram, dN/dE is the slope of the thick-target yield function in number of x rays per incident proton per keV, $S(E)$ is the stopping power in (keV cm²/g), $N(E)$ is the number of x rays observed per incident proton at energy E, and $\bar{\mu}$ is the mass-absorption coefficient of the target material for its own characteristic radiations.

The number of x rays produced per proton $N(E)$ is determined by counting all the pulses from the counter between two bias levels set to include all the pulses corresponding to the x rays. The slope dN/dE is determined graphically from the thick-target counting rate observed as a function of bombarding energy. Table I shows how $N(E)$ and dN/dE at a bombarding energy of 441 keV were obtained. The counting rate observed from each target is shown in column 4. The number of x rays emitted per microcoulomb is calculated by multiplying the observed counting rate by the transmission geometrical factor listed in column 5. For all the targets listed, the geometrical factor Ω was 1024. (The x rays are assumed to have an isotropic distribution.) The transmission factor A depends on the attenuation of the x rays produced at the target by the Mylar vacuum window, the air, and the beryllium window on the crystal. Absorption coefficients for carbon, oxygen, hydrogen, and beryllium were taken from McGinnies,[19] and for air from Compton and Allison.[20] The rapid decrease in A as the incident photon energy is decreased accounts for the increase in the numbers listed in this column as the atomic number decreases (or as x rays from higher shells are treated). The sixth column is obtained by dividing the product of the numbers listed in columns 4 and 5 by the number of protons in 1 μC. This yield is *not* corrected for

[19] R. T. McGinnies, Natl. Bur. Standards Circ. No. 583 (U. S. Government Printing Office, Washington, D. C., 1959), Supplement.

[20] A. H. Compton and S. K. Allison, *X-Rays in Theory and Experiment* (D. Van Nostrand and Company, New York, 1935).

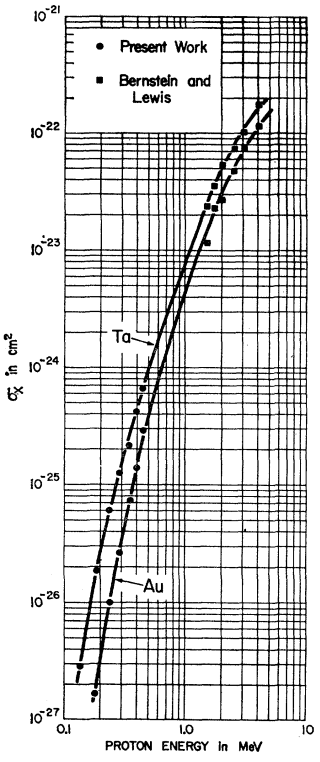

FIG. 3. The L x-ray production cross sections for tantalum and gold are plotted as a function of proton energy. The points between 1.5 and 4.0 MeV are those given in reference 5.

self-absorption of x rays in the target since this effect is included in the second term of Eq. (1) when the cross sections are evaluated.

Table II shows the x-ray production and the ionization cross sections obtained by using Eq. (1). The stopping powers $S(E)$ used to evaluate the first term were computed from available experimental data[21–23] by making reasonable extrapolations between materials with different atomic numbers. The absorption coefficients $\bar{\mu}$ were estimated from tables in references 19 and 20. In the extrapolation procedure, care was taken to make certain that the values below the appropriate absorption edge were used. In the case of oxide targets, both $S(E)$ and $\bar{\mu}$ were computed by using Bragg's rule. The procedure here is simply to add linearly the partial stopping powers due to the various target materials to obtain the total stopping power; and likewise from the absorption coefficients. The fluorescence yields of the K shells were taken from tables in "Nuclear Spectroscopy Tables."[24] The L-shell fluorescence yields are not well known in many cases. Estimates and extrapolations were made from existing data given by Wapstra *et al.*,[24] Burhop,[25] and Robinson and Fink.[26] In addition, some recent experimental values obtained by the authors[27] were used in certain cases. Except for uranium,[28] no data are available on M-shell fluorescence yields. The estimates given in Table II are based on systematics exhibited by the K- and L-shell yields. The relation between the x-ray production cross section σ_x, and the ionization cross section σ_I is

$$\sigma_x = \bar{\omega}\sigma_I, \tag{2}$$

where $\bar{\omega}$ is the average fluorescence yield for the appropriate atomic shell.

The experiment was carried out in two steps. First, the absolute x-ray yield from each target was measured using a proton bombarding energy of 441 keV—the $Li^7(p,\gamma)$ reaction resonance energy. Then the relative thick target yields were determined as a function of proton energy. The yield curves were then normalized to the 441 keV point and the x-ray production cross sections were computed using Eq. (1).

Because of the complex way in which the cross section depends on the observed counting rate, it is very difficult to assign meaningful standard errors to the final results. The best measurements are those for

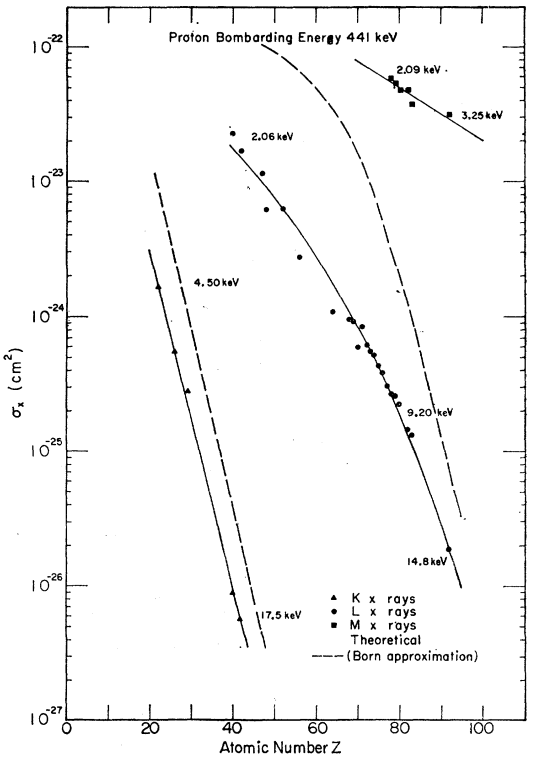

FIG. 4. The x-ray production cross sections for K, L, and M x rays as a function of atomic number (Z) are shown in this figure. A theoretical curve for L x-ray production using a plane-wave Born approximation is also shown. The numbers next to the curves indicate the approximate quantum energies of the particular x rays represented by the experimental points.

[21] M. Bader, R. E. Pixley, F. S. Mozer, and W. Whaling, Phys. Rev. **103**, 32 (1956).
[22] D. W. Green, J. N. Cooper, and J. C. Harris, Phys. Rev. **98**, 466 (1955).
[23] S. D. Warshaw and S. K. Allison, Revs. Modern Phys. **25**, 779 (1953).
[24] A. H. Wapstra, G. J. Nijgh, and R. van Lieshout, *Nuclear Spectroscopy Tables* (North-Holland Publishing Company, Amsterdam, 1959).
[25] E. H. S. Burhop, *The Auger Effect* (Cambridge University Press, New York, 1952).
[26] B. L. Robinson and R. W. Fink, Revs. Modern Phys. **32**, 117 (1960).
[27] See reference 18 and further work to be published shortly.
[28] H. Lay, Z. Physik **91**, 533 (1934).

TABLE III. Thick-target x-ray yields and x-ray production cross sections. The yields are given in x rays per proton and the cross sections in cm².

Element	Z	Atomic shell	$N(E)$ and σ_x	$E_p=200$ keV	$E_p=300$ keV	$E_p=400$ keV	$E_p=500$ keV
Uranium	92	M	$N(E)$	2.2×10^{-6}	8.5×10^{-6}	2.5×10^{-5}	6.1×10^{-5}
			σ_x	2.6×10^{-24}	8.5×10^{-24}	2.2×10^{-23}	5.0×10^{-23}
Lead	82	M	$N(E)$	1.3×10^{-5}	3.6×10^{-5}	7.0×10^{-5}	1.2×10^{-4}
			σ_x	9.0×10^{-24}	1.9×10^{-23}	3.2×10^{-23}	4.8×10^{-23}
Gold	79	L	$N(E)$	2.4×10^{-9}	5.8×10^{-8}	3.8×10^{-7}	1.8×10^{-6}
			σ_x	3.4×10^{-27}	3.8×10^{-26}	1.5×10^{-25}	4.1×10^{-25}
Tantalum	73	L	$N(E)$	2.4×10^{-8}	2.7×10^{-7}	1.2×10^{-6}	4.1×10^{-6}
			σ_x	2.6×10^{-26}	1.6×10^{-25}	4.6×10^{-25}	1.0×10^{-24}
Cadmium	48	L	$N(E)$	1.9×10^{-6}	8.3×10^{-6}	1.8×10^{-5}	4.0×10^{-5}
			σ_x	9.8×10^{-25}	2.2×10^{-24}	4.5×10^{-24}	9.0×10^{-24}
Molybdenum	42	L	$N(E)$	5.9×10^{-6}	2.3×10^{-5}	5.4×10^{-5}	1.1×10^{-4}
			σ_x	2.3×10^{-24}	6.8×10^{-24}	1.3×10^{-23}	2.2×10^{-23}
Zirconium	40	K	$N(E)$	1.7×10^{-10}	2.5×10^{-9}	1.4×10^{-8}	5.2×10^{-8}
			σ_x	1.2×10^{-28}	1.0×10^{-27}	4.0×10^{-27}	1.2×10^{-26}
Copper	29	K	$N(E)$	4.6×10^{-8}	2.9×10^{-7}	1.1×10^{-6}	3.3×10^{-6}
			σ_x	2.1×10^{-26}	7.1×10^{-26}	1.9×10^{-25}	4.7×10^{-25}
			[a] $N(E)$ Messelt	1.9×10^{-8}	2.4×10^{-7}	1.17×10^{-6}	...
			[a] σ_x Messelt	1.3×10^{-26}	8.6×10^{-26}	2.9×10^{-25}	...
			[b] σ_x Singh	...	...	1.6×10^{-25}	...
Titanium	22	K	$N(E)$	3.0×10^{-7}	1.6×10^{-6}	6.2×10^{-6}	2.0×10^{-5}
			σ_x	1.1×10^{-25}	4.7×10^{-25}	1.2×10^{-24}	2.1×10^{-24}

[a] See reference 9. [b] See reference 7.

the K and L x-ray transitions with the highest energies because the corrections for x-ray absorption are least important in these cases. For example, the attenuations in air, Mylar window, and beryllium window for molybdenum K x rays and bismuth L x rays are less than 1%. In addition, self-absorption in the target is not very large. [For molybdenum, the first term in Eq. (1) is about 70 times as large as the second for a proton-bombarding energy of 441 keV.] The ionization cross section $[\sigma_I(E)]$ measurements for the K x rays are most reliable, since only the K-shell fluorescence yields are well known. For the case of molybdenum, the standard error in $N(E)$ is $\pm10\%$ and in $\sigma_I(E)$ it is $\pm15\%$ at a proton-bombarding energy of 441 keV. For M x rays in platinum and L x rays in zirconium, the errors are very much larger. In these cases, the x rays are attenuated by more than a factor of 100 between the counter and the target. The self-absorption term in Eq. (1) is of the same order as the first term, and no measurements of the fluorescence yields are available. The measured values of $N(E)$ and $\sigma_x(E)$ are probably accurate to a factor of 2, and the ionization cross section σ_I is only an order of magnitude estimate.

IV. DISCUSSION OF RESULTS

The dependence of the L x-ray production cross section in Ta and Au on the proton bombarding energy is shown in Fig. 3. The high-energy points in each case are taken from reference 5. The two cross sections at 4.00 MeV differ by less than a factor of 2, whereas at 0.20 MeV they differ by more than an order of magnitude. This observation is similar to the behavior of the K-shell cross sections for which the shells having a higher average ionization potential have cross sections with a steeper dependence on the proton bombarding energy. The high-energy points are in good agreement with theoretical calculations based on the plane-wave Born approximation as given in reference 13. (In this calculation, the L-shell screening constant θ_L is used as a parameter to fit the data.) At lower energies, the calculations are not in accord with the experimental data for reasons which will be discussed shortly.

Table III shows a summary of thick-target x-ray yields and x-ray production cross sections as a function of proton energy for a number of representative elements. The yields and cross sections for copper K x rays obtained by Singh[7] and Messelt[9] are also shown for comparison. The agreement between the previous measurements and the present values is reasonably good. Additional comparisons are shown in Tables I and II for the K-shell ionization cross section of Mo. The agreement between the two measurements for this element is not as good as in the case of copper.

The x-ray production cross sections at a proton bombarding energy of 441 keV as a function of atomic number (Z) are shown in Fig. 4. The L and M x-ray curves have a Z dependence which is not as steep as the K x-ray curve. The theoretical curve for L x-ray yields shown in Fig. 4 was obtained following the methods outlined in reference 13. The same screening constants (θ_L) used to fit the data obtained at higher bombarding energies were employed in these calculations. The theoretical x-ray production cross sections were computed from the ionization cross sections using the fluorescence yields given in Table II. It is evident

from the discrepancy between the theoretical curve and the experimental results that the plane-wave Born approximation is not applicable at low bombarding energies. At higher energies (between 1.5 and 4.0 MeV) this approximation works quite well.[13] To explain the low-energy data it is probably necessary to include effects due to the Coulomb deflection of the bombarding particle by the nuclear field. It has already been shown[14] that this must be done to fit the K x-ray ionization cross sections at low bombarding energies. No theoretical expressions for M-shell ionization cross sections are available so that no quantitative comparison can be made.

ACKNOWLEDGMENTS

The authors would like to thank Roy Cedarlund, Bruce Burford, and Al Horn for their help during the course of these experiments.

PHYSICAL REVIEW VOLUME 127, NUMBER 5 SEPTEMBER 1, 1962

Accurate Analytical Self-Consistent Field Functions for Atoms. II. Lowest Configurations of the Neutral First Row Atoms

E. CLEMENTI
Research Laboratory, International Business Machines Corporation, San Jose, California
AND
C. C. J. ROOTHAAN AND M. YOSHIMINE*
Laboratory of Molecular Structure and Spectra, Department of Physics, University of Chicago, Chicago, Illinois
(Received April 23, 1962)

Self-consistent field wavefunctions have been obtained for the ground states of the first row atoms and for the excited states belonging to the same configurations. They are the solution of the variational problem of finding the best orbitals for a given state, without any additional approximations except for those inherent in the expansion method.

INTRODUCTION

ANALYTICAL self-consistent field (SCF) functions for the $1s^2$, $1s^22s$, and $1s^22s^2$ atomic configurations were published recently.[1] These calculations, which we shall now consider (I) in a series of papers,[2] differ from other recent work[3–5] in, among other things, that a great deal of effort has been put into obtaining *accurate representations* of the Hartree-Fock functions with

TABLE I. Orbital exponents of the basis function.

	Li(^2S)	Be(^1S)	B(^2P)	C(^3P)	C(^1D)	C(^1S)	N(^4S)
1s	2.4803	3.4703	4.4661	5.4125	5.4300	5.3842	6.4595
1s	4.7071	6.3681	7.8500	9.2863	9.1500	9.0600	10.8389
2s	0.3500	0.7516	0.8320	1.0311	1.2255	1.2100	1.4699
2s	0.6600	0.9084	1.1565	1.5020	1.6142	1.5929	1.9161
2s	1.0000	1.4236	1.9120	2.5897	2.6990	2.5964	3.1560
2s	1.7350	2.7616	3.5213	4.2595	4.2131	4.2500	5.0338
2p			0.8783	0.9554	0.9372	1.1060	1.1937
2p			1.3543	1.4209	1.4147	0.5074	1.7124
2p			2.2296	2.5873	2.5545	2.3590	3.0112
2p			5.3665	6.3438	6.3021	6.2000	7.1018
	N(^2D)	N(^2P)	O(^3P)	O(^1D)	O(^1S)	F(^2P)	Ne(^1S)
1s	6.4730	6.5035	7.6160	7.6105	7.5333	8.5126	9.5735
1s	10.9700	1.1318	13.3243	13.2681	12.7015	14.4130	15.4496
2s	1.2745	1.2721	1.7582	1.7582	1.7098	1.8599	1.9550
2s	1.8034	1.8038	2.5627	2.5630	2.4512	2.7056	2.8462
2s	3.1159	3.0120	4.2832	4.2754	4.0761	4.9019	4.7746
2s	5.0338	5.2338	5.9445	5.9445	5.9445	6.4440	7.7131
2p	1.0906	1.0580	1.1536	1.0626	1.0555	1.2655	1.4700
2p	1.6446	1.6279	1.7960	1.7405	1.6985	2.0301	2.3717
2p	3.0200	3.0243	3.4379	3.4198	3.3517	3.9106	4.4545
2p	7.1650	7.2029	7.9070	7.8890	7.6690	8.6363	9.4550

* Present address: Argonne National Laboratory, Argonne, Illinois.
[1] C. C. J. Roothaan, L. M. Sachs, A. W. Weiss, Revs. Modern Phys. **32**, 186 (1960).
[2] In reference 1, we referred tothe paper describing the general theory (here reference 6, as I). We hereby specifically withdraw this and we shall use the Roman numerals to indicate the various practical applications which are now under way or planned for the near future.
[3] L. C. Allen, J. Chem. Phys. **34**, 1156 (1960).
[4] R. E. Watson and A. J. Freeman, Phys. Rev. **123**, 521 (1961); **124**, 1117 (1961).
[5] L. M. Sachs, Phys. Rev. **124**, 1283 (1961).